Academic Journal of Science and Technology
ISSN: 2771-3032 | Vol. 14, No. 1, 2025

The Impact of the Angle Between the Soft-Hard Interlayer Rock Mass and the End Anchorage of Bolts on the Support Stress Field

Haojie Li[1], Weimin Liang[1, *]

[1] School of Civil Engineering, Henan Polytechnic University, Jiaozuo 454100, China

[*] Corresponding author: Haojie Li (Email: LihaojieHPU@163.com)

Abstract: To investigate the impact of the angle between the soft-hard interlayer rock mass and the end-anchored bolts on the support stress field, numerical simulations were conducted to create models of soft-hard interlayer rock masses with varying dip angles. The distribution of the support stress field was analyzed. The results show that the variation in the angle between the soft-hard interlayer rock layers and the end-anchored bolts significantly affects the support stress field at the anchorage. In all models, the anchorage section is under tension, while the areas below the anchorage and above the bearing plate are under compression. In the single-bolt support model, when the angle between the rock layers and the bolt is small, the stress field is uniformly symmetrical, with a larger compression stress area and a symmetrical tension stress area. As the dip angle increases, the stress field gradually develops into an asymmetric distribution, with the compression stress area shifting and the tension stress area becoming asymmetric. The compression stress in the soft rock layers is lower than that in the hard rock layers. In the double-bolt support model, the overlapping stress field gradually transitions from a uniform symmetrical distribution to an asymmetric one as the dip angle increases. The internal stress values gradually decrease, and the actual support effectiveness weakens. It is evident that the angle between the soft-hard interlayer rock mass and the end-anchored bolts has a significant impact on the support stress field. The findings of this study provide useful insights for the design and construction of bolt support systems, including the spacing between bolts, in engineering practice.

Keywords: End Anchorage, Stratified Rock Mass, Support Stress Field, Similarity Simulation, Numerical Simulation.

1. Introduction

Since 1956, the use of anchor bolt support in tunnels has become widespread in various mining applications, and over the past 60 years, it has become the most commonly used support method in many mines [1, 2]. The stress field is central to the study of tunnel surrounding rock deformation and failure, as well as the interaction between support and surrounding rock [3]. To better quantify the supporting effect of the support system on the surrounding rock, the concept of the support stress field was introduced [4]. Through a comprehensive analysis of the stress distribution in the support system, the accuracy and scientific nature of support design and construction were enhanced. In this template, the "Styles" menu should be used to format your text if needed. Highlight the text you want to designate with a certain style, and then select the appropriate name on the Style menu. The style will adjust your fonts and line spacing. Use italics for emphasis; do not underline as shown in Table 1.

The support stress field is closely related to factors such as prestress, angle, and density [5, 6]. Both domestic and international scholars have conducted extensive research on these factors. Zi Xin [7] analyzed the stress distribution of tunnel surrounding rock under the action of single bolts and bolt groups, based on laboratory tests and numerical simulations. Zhou Yiqun et al. [8] studied the distribution of prestress in end-anchored support under different soft-hard stratified conditions using numerical simulations. The results showed that high prestress can effectively increase the range of the compression stress area. Lin Jian [9] set up a large-scale anchor bolt support experimental platform and found that the support stress field in space approximates a "pomegranate" shape, with two compression stress areas and one tension stress area forming at the two ends of the free section and the anchorage section, respectively. These findings are consistent with those of Wang Jinhua [10]. Li Jianzhong et al. [11] proposed a reasonable method for obtaining the anchor bolt support stress field, finding that compared to support density, the pre-tension force has a greater impact on the support stress field. Wei Sijiang [12] showed through numerical simulations that the stress field in the rock mass around the anchorage body takes a spindle shape, with a conical distribution at the start of the anchorage. Kang Hongpu [13] used numerical simulations and underground tests to demonstrate that high prestress can expand the compression stress area and enhance the active support effect. Li Fengzhen [14], using the same method, found that using larger protective components can effectively expand the compression stress area of the anchor bolts. Shi Yao [15] further studied and found that π-shaped steel bands are more beneficial for stress field expansion compared to other components. Duan Hongmin [16] discussed the design methods for tunnel roof support and optimized the support methods for mining shaft shafts.

Tunnel surrounding rock is often layered, and research on layered rock masses should be fully referenced. Zhao Pinglao [17] studied the constitutive relationship of layered rock masses, and He Zhongming [18] improved it through uniaxial compression tests. Li Shenzhen [19] and Chu Chaohong [20], based on this, focused on their anisotropic characteristics. Wei Chuanwen [21] used numerical simulations to study the caving mechanism of layered surrounding rock in tunnels. Based on existing constitutive models, Yang Yanyi [22] and Yang Songlin [23] studied the anchorage mechanism and constitutive models of layered rock masses. Zhang Junru [24] studied

support measures for inclined layered rock masses and found that setting anchor pipes at vertical interfaces effectively transfers the bias loading. Ge Xiurun [25] showed that anchor bolts can significantly improve the shear strength of joint surfaces in layered rock masses, and Cao Xingsong [26] optimized anchor bolt support for inclined rock layers. Furthermore, since tunnel surrounding rock often exhibits characteristics of soft-hard interlayers, Yang Fan [27] studied the failure mechanism and support technology of soft-hard interlayer surrounding rock, and Zhang Lixin [28] examined its deformation characteristics. Pang Weijun's research [29] indicated that when the angle between the rock layers and tunnel direction is less than 30 degrees, tunnels primarily undergo asymmetric deformations along the layers. On this basis, Guo Qinghao [30] found that support around surrounding rock should be enhanced where soft rock occupies a larger proportion.

Given the relative scarcity of research on the influence of the angle between the soft-hard interlayer rock mass and the end-anchored bolts on the support stress field, this paper develops four models of soft-hard interlayer rock masses with varying angles between the layers and bolts. The support stress field distribution is measured using built-in sensors, and numerical simulation software is employed for modeling and analysis, aiming to provide deeper insights into the support stress field.

2. Model Design

Given that the main focus of this study is on the impact of the angle between the anchor bolts and the rock mass on the support stress field, the angle is treated as the key variable in the experimental setup. To ensure experimental operability and repeatability, the model dimensions (length × width × height) are set to 0.4 × 0.4 × 0.8 m, with the design incorporating soft-hard interlayers. The distance between each layer is fixed at 0.2 m. The anchor bolts are arranged vertically at the center of the model, perpendicular to the ground.

To fully investigate the impact of the angle between the rock mass and the anchor bolts on the support stress field, four angle values of 90°, 60°, 45°, and 0° were selected for the experiment. An angle of 90° means that the layers are parallel to the ground, with the anchor bolts perpendicular to the rock mass. Angles of 60° and 45° simulate mildly and moderately inclined rock masses, respectively, to assess the anchoring effect under these two common conditions. When the angle is 0°, the layers are parallel to the anchor bolts, which is used to test the load-bearing capacity and stability of the anchoring system under extreme conditions. The model design diagram is shown in Figure 1, where α represents the complementary angle between the anchor bolt and the rock mass.

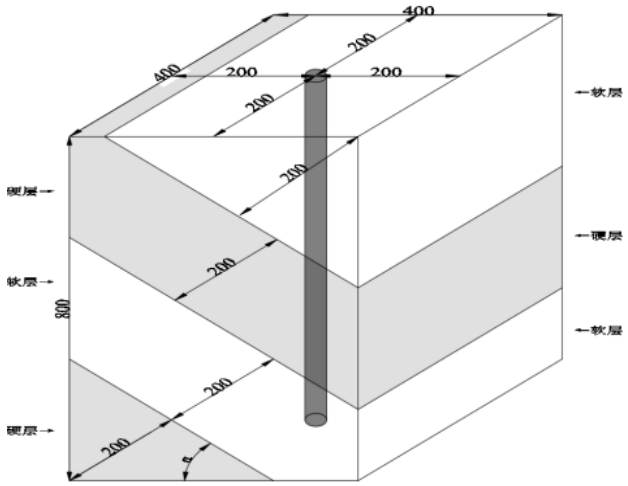

Figure 1. Support Stress Field Testing Model (Unit: mm)

After referring to existing literature [31] and conducting multiple experimental mix ratio tests (as shown in Figure 2), the material mix ratio for the hard layer of the model was determined as cement: fine sand: gypsum: water = 1:0.5:0:0.4, and for the soft layer, the mix ratio was cement: fine sand: gypsum: water = 1:10:9:7. The mechanical properties of the materials are shown in Table 1.

Figure 2. Rock Mass Mix Ratio Experiment

Table 1. Mechanical Properties of Soft and Hard Layers

Item	Mechanical Parameter	Value
Soft Layer	Elastic Modulus/GPa	2.1
	Poisson's Ratio	0.19
	Compressive Strength/MPa	25
	Tensile Strength/MPa	4
	Internal Friction Angle /°	35.6
Hard Layer	Elastic Modulus/GPa	3.7
	Poisson's Ratio	0.13
	Compressive Strength/MPa	31
	Tensile Strength/MPa	8
	Internal Friction Angle /°	40

The experimental anchor bolts used were HRB400 hot-rolled threaded steel, with a diameter of 22 mm and a length of 1500 mm. The central 800 mm of the bolt was located

inside the model, with 350 mm extending above and below the model. The top of the anchor bolt was fixed, and the upper 200 mm that extended into the model was anchored using resin anchoring agents. The square bearing plate at the bottom was made of 45# steel, with dimensions of 160 × 160 × 10 mm.A pre-stress of 135 kN was applied to the anchor bolt.

3. Simulation Results of the Anchor Bolt Support Stress Field

3.1. Support Stress Field of a Single Anchor Bolt Support

Considering the initial stress state of the model and existing literature [5, 8], a compressive stress of 0.1 MPa was set as the boundary of the support stress field. The region where the compressive stress induced by the support exceeds 0.1 MPa is considered the support stress field, and the 0.1 MPa compressive stress contour line represents the boundary of the stress field.

The inclined layering of the model is parallel to the XOZ plane. A section cut in the XOZ plane can more intuitively reflect the impact of the angle between the anchor bolt and the rock mass on the distribution of the support stress field. In contrast, on the section parallel to the YOZ plane, the rock mass properties are uniform at the same height, and each layer of rock is perpendicular to the anchor bolt. The support stress field is similar to the "gourd" shape shown in Figure 3, which is symmetrical with respect to the anchor bolt, and thus, it cannot show the influence of the angle between the anchor bolt and the rock mass.

Therefore, for the four models, a section was made in the XOZ plane, as shown in Figure 4, to study the effect of the rock mass and anchor bolt angle on the support stress field.

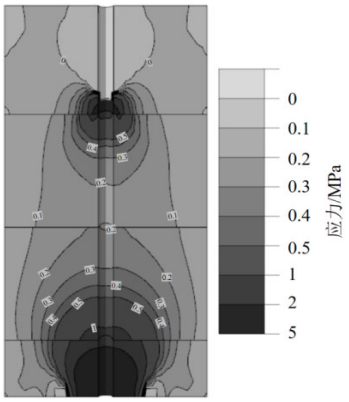

Figure 3. Support Stress Field in the YOZ Plane Section of Model 3

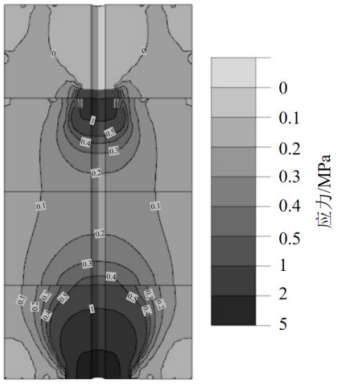

(1) Anchor Bolt Perpendicular to the Rock Mass (Model 1)

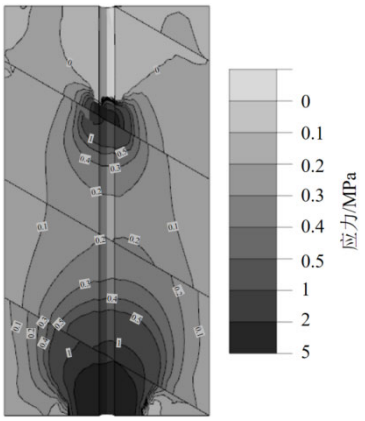

(2) Anchor Bolt at a 60° Angle to the Rock Mass (Model 2)

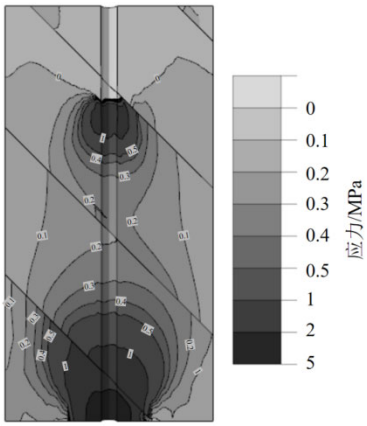

(3) Anchor Bolt at a 45° Angle to the Rock Mass (Model 3)

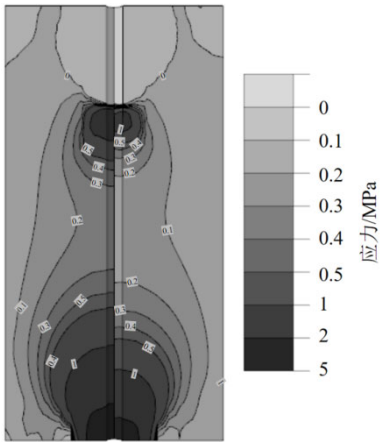

(4) Anchor Bolt Parallel to the Rock Mass (Model 4)

Figure 4. Support Stress Field of the Single Anchor Bolt Model

As shown in Figure 4, the angle between the anchor bolt and the rock mass has a significant impact on the distribution pattern of the support stress field. The stress contours in all models shift at the interfaces between the layers, indicating that the layered interface has a relatively weak stress transfer capacity. For clearer analysis of the stress field distribution, the width of the support stress field along the X-axis is denoted as b, and the height along the Z-axis as h. It is evident that the angle between the anchor bolt and the rock mass, as well as the rock layer properties, significantly affect both the overall shape and internal stress distribution of the support stress field. This influence is manifested in the following two points:

Model 1: The support stress field is perfectly symmetrical. The external contour forms a "gourd" shape that first widens and then narrows from top to bottom. The upper convex area

overlaps with the bottom of the anchoring section. The width b reaches its maximum value of 0.63b at 0.5 m from the bottom, and the minimum width of the middle section is 0.6b. The concave region at 0.25h from the bottom is the widest, with a width of 0.8b. The internal compressive stress zone of 0.2 MPa is split into two separate regions. The region above the bearing plate reaches a maximum width of 0.7b, which is 50% larger than the area below the anchoring section.

The effect of the layering on the stress field in Model 1 is relatively weak. As the stress field passes through the layer interfaces, the width of the lower layer increases compared to the upper layer. The overall distribution remains symmetrical, with a relatively large compressive stress zone. The anchor bolt's perpendicular alignment with the rock mass reduces the dispersive effect of the supporting force in the rock mass, thus expanding the area of the support stress field.

Model 2 (Angle of 60°): As the angle between the anchor bolt and the rock mass decreases to 60°, the symmetry of the stress field decreases. The overall shape becomes "spindle-shaped," and the stress field tilts upward along the interface with the ground. The upper convex part of the support stress field narrows to 0.6b, and after the first two layer interfaces, the stress field shifts downward due to the mechanical property differences between the layers and the angle of the interfaces. The width is similar to that of Model 1. After the third interface, the significant stiffness difference between soft and hard layers results in more uniform stress transfer at the interface, which reduces the concentrated high pre-stress and causes the compressive stress zone in the bottom hard layer to expand. The stress field shifts toward the upper left and extends toward the model's edge, with the maximum width increasing by 18% compared to Model 1, and the region where the compressive stress exceeds 0.2 MPa increasing by 5%. Furthermore, the inclined angle increases the shear stress component along the tilt direction, which causes the area of the tensile stress zone in the anchoring section to increase by approximately 20%, and the stress field is no longer symmetric with respect to the anchor bolt.

Model 3 (Angle of 45°): With further reduction in the angle between the anchor bolt and the rock mass, the stress field becomes asymmetrical, with a higher left side and a lower right side, tilting downward along the inclination of the rock mass. The external contour of the upper part of the stress field in the model is similar to Model 1, but the lower part extends over the entire cross-section at 0.13h from the bottom. The internal compressive stress zone of 0.2 MPa connects the hard layers in the middle of the model and changes from two separate areas in Model 1 to an eccentric "gourd" shape. The narrowest point is 0.18b at 0.5h from the bottom. The stress field continues to shift downward along the interface and connects with the lower soft layer. The soft rock below, affected by both the bearing plate and the overlying hard rock, has a relatively larger 0.2 MPa compressive stress zone. The right edge of the stress field moves downward along the interface for the first two layer crossings, while the left edge shifts upward by 0.02 m after the third layer crossing due to the soft-hard rock layer differences. The compressive stress in the adjacent regions of the upper soft rock and lower hard rock increases by 0.1 MPa, and the area of the compressive stress zone increases.

Model 4 (Anchor at Soft-Hard Layer Interface): In Model 4, where the anchor bolt is placed at the soft-hard layer interface and the bearing plate acts uniformly on both layers, the stress field is heavily influenced by the stiffness differences between the soft and hard layers. The hard layer, with higher stiffness, deforms less and quickly transfers the applied force over a larger area. In contrast, the soft layer, with lower stiffness, deforms locally, absorbing the applied force and concentrating the support stress field in a smaller region, reducing the overall area compared to the hard layer.

Specifically, in Figure 4(4), the stress field contour on the hard layer side forms a semi-bottle shape that gradually widens from top to bottom. At 0.15h from the top, the width is 0.2b, and it reaches its maximum width of 0.45b at 0.2h from the bottom, covering 90% of the left side of the anchor bolt. The internal 0.2 MPa compressive stress zone forms a semi-gourd shape, with the width at the top at 0.33h being 0.25b, the middle narrowing to 0.18b, and the bottom expanding to 0.38b. In contrast, the stress field contour on the soft layer side forms a gourd shape, with the internal 0.2 MPa compressive stress zone split into two parts: one below the anchoring section with a length of 0.18h in the Z-axis direction, resembling a half-circle with a diameter of 0.09h; and the other above the bearing plate, with the highest point at 0.35h from the bottom of the model. Additionally, as the distance from the bottom of the model increases from 0.05h to 0.39h, the spacing between the 0.2 MPa compressive stress contours in the soft and hard layers increases to 0.13h. After this, the spacing decreases to 0.02 m as the distance from the bottom of the model increases from 0.58h to 0.7h.

Among the four single-anchor bolt support models, Model 1 demonstrates a typical symmetrical "gourd" shaped stress field. As the layering angle and stiffness differences increase, Models 2 and 3 show a transition to an asymmetric distribution of the stress field. The stress concentration effect at the soft-hard layer interface becomes more evident, limiting the support range of the anchor bolt. Model 4 shows a clear difference in stress field size between the soft and hard layers, with reduced support efficiency. It is evident that rock layer properties, the angle between the rock mass and the anchor bolt, and the rock mass layering significantly influence the morphology of the support stress field. As the angle between the rock mass and the anchor bolt decreases, the anchor density should increase, and the spacing should decrease. When the angle approaches 0°, a single anchor bolt can no longer ensure the stability of the rock mass, and combined methods such as grouting and shotcrete should be used.

3.2. Double Anchor Bolt Support Stress Field

The support stress field edge for a single anchor bolt model is located 0.16-0.18 meters away from the anchor. Therefore, it can be assumed that when the distance between two anchor bolts does not exceed 0.32 meters, the support stress fields will overlap. Based on previous experimental and numerical simulation results, a double-anchor bolt support model with an anchor bolt spacing of 0.3 meters is established to study the effect of the angle between the rock mass and the anchor bolt on the superposition of the support stress field.

The model design is shown in Figure 5. In the figure, α represents the complementary angle between the anchor bolt and the rock mass. The interlayer spacing remains at 0.2 meters, and the anchor bolt positioning is unchanged. The gray rock layers represent hard layers, and the white rock layers represent soft layers.

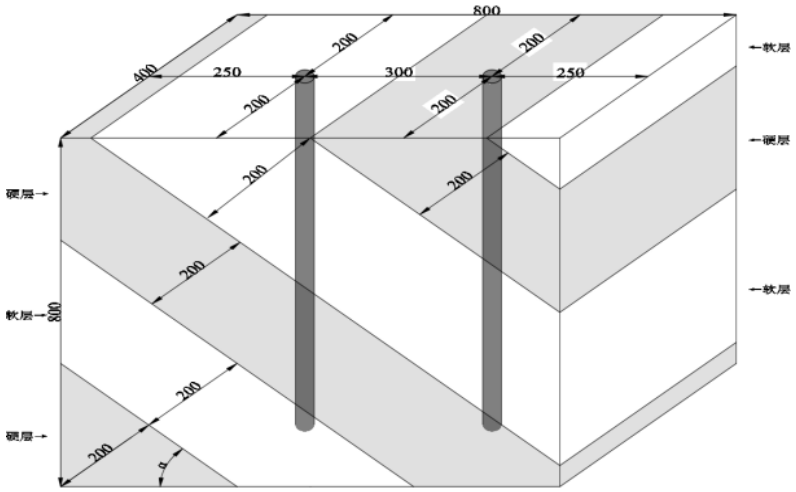

Figure 5. Support Model Design Diagram (Unit: mm)

Similar to the single-anchor bolt support model, a 0.1 MPa compressive stress is chosen as the boundary for the support stress field. The angles between the anchor bolt and the rock mass are set to 90° (anchor bolt perpendicular to the rock mass), 60°, 45°, and 0° (anchor bolt parallel to the rock mass). When applying a pre-stress of 135 kN to the four models, the support stress field contour maps in the XOZ plane are shown in Figure 6.

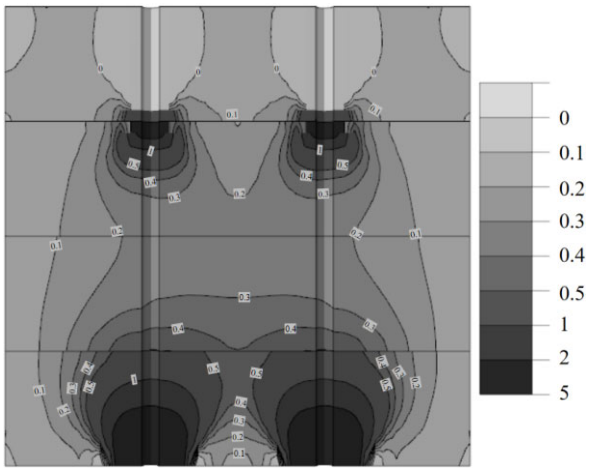

(1) Anchor bolt and rock mass angle perpendicular (Model 5)

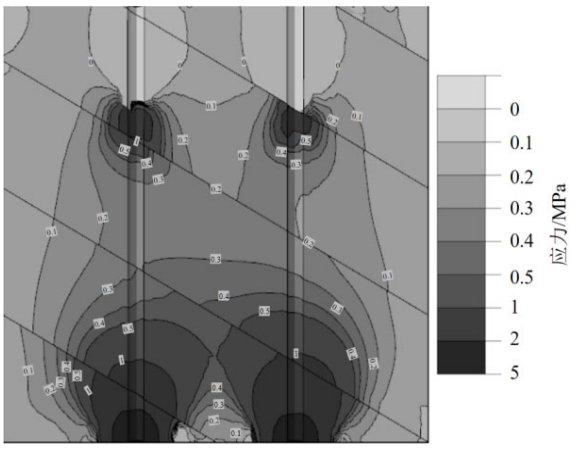

(2) Anchor bolt and rock mass angle 60° (Model 6)

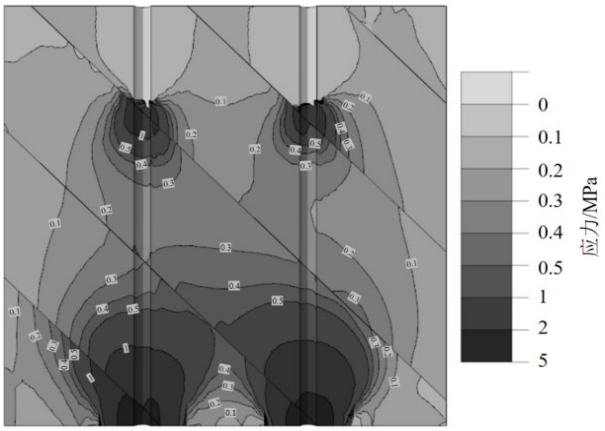

(3) Anchor bolt and rock mass angle 45° (Model 7)

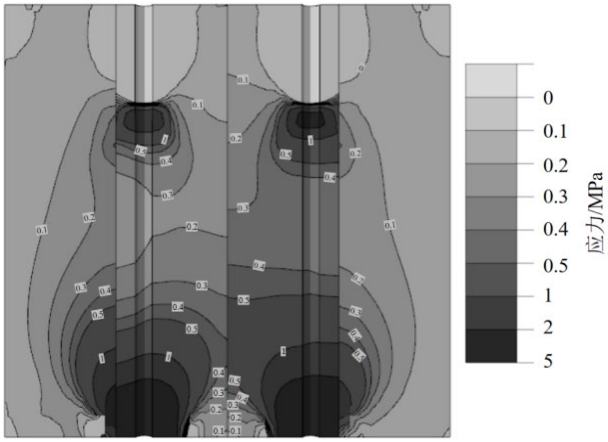

(4) Anchor bolt and rock mass angle 0° (Model 8)

Figure 6. Support Stress Field of the Double-Anchor Bolt Support Model

From Figure 6, it can be observed that the support stress fields of the two anchor bolts in each model overlap in the central region of the model. The angle between the anchor bolt and rock mass, as well as the stratification properties of the rock mass, significantly influence the overlapping range of the support system. As the angle between the anchor bolt and rock mass increases, the symmetry of the support stress field gradually decreases. Let the height of each model be denoted as h, where h = 0.8 m, and the width as b, where b = 0.8 m in this section.

Model 5 (Anchor bolt and rock mass angle 90°):

The support stress field is symmetrical about the central region of the model, with an external contour resembling a rounded rectangle. The compressive stress area appears at a distance of 0.8h from the bottom of the model, with an initial width of about 0.63b, gradually increasing downwards. The maximum width occurs at the interface between the soft and hard rock layers, reaching 86% of the model's width. The Z-axis length is larger on both sides, with the smallest length in the central part of the model, reaching 0.73h. The internal 0.2MPa stress region forms an "X" shape, with the largest width being 0.63b below the anchorage section, narrowing to 0.5b in the middle, and reaching 0.8b above the bearing plate. The compressive stress region near the bearing plate is significant, with a 0.3-0.5MPa stress area that is connected as a whole, indicating a sufficient overlap of the high-stress region of the two anchor bolts in the middle and lower parts of the model. The 0.1MPa compressive stress area covers 65% of the area of the lower three rock layers, fully covering the central region of these layers, providing relatively effective support to the rock mass.

Model 6 (Anchor bolt and rock mass angle 60°):

The overall support stress field is tilted upwards along the angle between the rock mass and the surface. The upper boundary of the central part is asymmetrical, showing a "left low, right high" pattern. The overall height increases by 6% compared to Model 5. The maximum width above the bearing plate reaches 0.88b, forming a more trapezoidal shape, with the area increasing by 5% compared to Model 5. The 0.1MPa compressive stress area covers the middle and lower parts of the model. Due to the stratification and inclination, the symmetry of the stress field decreases, and the stress distribution between the soft and hard layers becomes more uneven. Similar to Model 2, the stress area in the hard rock on the lower left is larger than in the adjacent soft rock. The stress at the interface between the layers increases by 0.1MPa compared to the adjacent soft rock. The internal 0.2MPa compressive stress area on the left side of the model is 1.2 times the area on the right side. The boundary on the upper side of the central part tilts downward along the stratification line, and the concave part of the right upper protrusion reaches the free section of the anchor bolt. The width is reduced by 10% compared to Model 5, and the overall area decreases by 10%, indicating that the support stress field has weakened, especially in the right half of the model.

Model 7 (Anchor bolt and rock mass angle 45°):

As the angle decreases to 45°, the stress path within the rock mass becomes longer, with greater attenuation during transmission. The effective normal stress component decreases, and the stress is distributed more in the tangential direction, reducing the strengthening effect on the surrounding rock. The larger angle increases the concentration of stress inside the rock mass. Compared to Model 5, the maximum width of the support compressive stress field decreases by 8%, and the overall area decreases by 15%. The external contour of the stress field deviates more clearly along the stratification line. This indicates that the stratification interface enhances the guidance of stress transmission, limiting the diffusion of prestress within the rock mass and reducing the effective range. At the same time, the stratification angle weakens the normal stress component, which reduces the external contour range compared to horizontally stratified models. The 0.2MPa compressive stress area is lowered in the middle part of the model, and at the right anchor bolt, it also shifts leftward to the free section of the anchor bolt. The minimum width decreases by 12% compared to Model 5, and the area covers 45% of the section. This shows that the decrease in angle disrupts the uniform transmission of stress, causing it to concentrate in localized areas and forming uneven stress distribution. Similar to Model 6, the stress field in the lower left corner of Model 7 expands to the model's edge, and the stress value increases by 0.1MPa compared to the adjacent soft rock. The 0.3MPa stress region in the central hard rock layer also significantly increases compared to the adjacent soft rock, indicating that decreasing the angle reduces the normal stress component, exacerbating the stress differences between the soft and hard layers.

Model 8 (Anchor bolt and rock mass angle 0°):

In this model, the soft and hard layers are alternately distributed vertically, and the distribution of the support stress field varies significantly between layers. The model is numbered from left to right as layers 1 to 4, with layers 1 and 3 being hard rock and layers 2 and 4 being soft rock. The stress field in layers 1 and 4 is similar to the hard and soft layers of Model 4, with an external contour approximately symmetrical about the center of the model. The width gradually increases from top to bottom, reaching 88% of the model's width at a distance of 0.25h from the bottom. The compressive stress field in layer 2 gradually decreases along the X-axis, showing a "trumpet" shaped distribution that is narrow on the right and wide on the left. At the interface with layer 3, the length is minimized, only 68% of the model's height. The 0.2, 0.3, and 0.4MPa contour lines in layer 3 show a "trumpet" shaped distribution, being narrow on the left and wide on the right. Due to the alternating distribution of soft and hard layers and differences in stiffness, the support stress field in the hard rock layers has a larger area and higher stress value compared to the soft rock layers. The 0.1MPa compressive stress area is similar to that of horizontally stratified models, but the 0.2MPa stress area is the smallest among the four models. This shows that vertical stratification and stiffness differences limit the interlayer transmission of stress, leading to a weak anchor bolt support effect. Even if the anchor density is increased, the support effect is still inadequate, and combined use with methods such as sprayed concrete or grouting reinforcement is necessary to achieve joint support.

4. Conclusion

(1) The Influence of the Angle Between Rock Mass and Anchor Bolt on the Distribution and Overlap of the Support Stress Field: The angle between the anchor bolt and the rock mass has a significant effect on the distribution and overlap range of the support stress field. In the case of a single anchor bolt with the rock mass perpendicular to the anchor bolt, the support stress field is evenly distributed and symmetric, with the external contour resembling a "gourd" shape, and both tensile and compressive stress areas being symmetric with respect to the anchor bolt. As the angle decreases, the tensile and compressive stress areas gradually become asymmetrical, with the area of the compressive stress zone in the middle expanding while the upper region shrinks. In such cases, increasing the anchor bolt density is recommended. When the rock mass is parallel to the anchor bolt, the compressive stress concentrates in a smaller range around the anchoring section and the bearing plate, resulting in localized support effectiveness. In these cases, it is necessary to consider

combined support methods such as sprayed concrete and grouting.

(2) The Effect of Anchor Bolt Inclination on the Overlap and Shape of the Support Stress Field in Double Anchor Bolt Systems: In the case of double anchor bolt support, the inclination angle has a more pronounced impact on the overlap range and shape of the support stress field. When the anchor bolts are perpendicular to the rock mass, the overlapping support stress field is evenly distributed and symmetric. As the angle between the anchor bolts and the layers decreases, the overlap region transitions into an asymmetric distribution, with internal stress values gradually decreasing. Additionally, the difference in stiffness between layers limits the efficiency of stress transfer, leading to reduced support effectiveness. In such cases, it is advisable to moderately increase the anchor bolt density. When the anchor bolts are parallel to the layers, significant differences in the stress distribution between soft and hard rock layers are observed, and the single anchor bolt support system performs poorly. In such conditions, combined support methods such as anchor cables, grouting, and sprayed concrete should be considered to ensure the stability of the rock mass.

(3) Further Research on the Influence of Layer Spacing and Anchorage Length on the Support Stress Field: In this study, the layer spacing and anchorage length are kept constant across all models. However, the influence of variations in layer spacing and anchorage length on the support stress field warrants further investigation. More in-depth research is needed to understand how changes in these parameters affect the overall support system and the distribution of stresses in different geological conditions.

References

[1] H. Kang, “Seventy years development and prospects of strata control technologies for coal mine roadways in China,” Chinese Journal of Rock Mechanics and Engineering, vol. 40, no. 1, pp. 1-30, 2021.

[2] H. Kang, “Development and prospects of support and reinforcement materials for coal mine roadways,” Coal Science and Technology, vol. 49, no. 4, pp. 1-11, 2021.

[3] H. Kang, P. Jiang, and J. Cai, “Test and analysis on stress fields caused by rock bolting,” Journal of China Coal Society, vol. 39, no. 8, pp. 1521-1529, 2014.

[4] H. Kang, “Analysis on types and interaction of stress fields in underground coal mines,” Journal of China Coal Society, vol. 33, no. 12, pp. 1329-1335, 2008.

[5] H. Kang, T. Jiang, and F. Gao, “Design for pretensioned rock bolting parameters,” Journal of China Coal Society, vol. 33, no. 7, pp. 721-726, 2008.

[6] H. Kang, “Research and Practice on the Integrated Technology of Bolt Support for Coal Roadways,” Journal of Rock Mechanics and Engineering, vol. 5, pp. 161-166, 2005.

[7] X. Z., B. Wang, W. Yu, et al., “Distribution Characteristics of Prestressed Field of End-Anchored Bolts,” Tunnel Construction, vol. 43, no. 10, pp. 1750-1759, 2023.

[8] Y. Zhou, J. Lin, Z. Wang, et al., “Study on Prestress Field Distribution Law of End Anchoring Rock Bolt in Combination Rock,” Coal Mining Technology, vol. 22, no. 6, pp. 46-49, 2017.

[9] J. Lin, Y. Shi, Z. Sun, et al., “Large scale model test on the distribution characteristics of the prestressed field of end-anchored bolts,” Chinese Journal of Rock Mechanics and Engineering, vol. 35, no. 11, pp. 2237-2247, 2016.

[10] J. Wang, H. Kang, and F. Gao, “Numerical simulation on load-transfer mechanisms and stress distribution characteristics of cable bolts,” Journal of China Coal Society, vol. 33, no. 1, pp. 1-6, 2008.

[11] J. Li, H. Kang, F. Gao, et al., “Analysis of the Stress Field of Anchor Support under the Influence of the Original Rock Stress Field and Its Effects,” Journal of Coal Science and Engineering, vol. 45, no. S1, pp. 99-109, 2020.

[12] S. Wei and B. Li, “Formation and Instability Modes of Anchorage Bodies under Prestressed Bolts,” Journal of Coal Science and Engineering, vol. 38, no. 12, pp. 2126-2132, 2013.

[13] H. Kang, T. Jiang, and F. Gao, “The Role of Prestress in Bolt Support,” Journal of China Coal Society, vol. 33, no. 7, pp. 680-685, 2007.

[14] F. Li, “Anchor prestress field distribution characteristics and support optimization of multi type composite roof,” China Mining Magazine, vol. 29, no. 9, pp. 97-103, 2020.

[15] Y. Shi, “Experimental study on stress distribution law of different bolt surface protection components,” Coal Engineering, vol. 55, no. 12, pp. 134-140, 2023.

[16] H. Duan, “Optimization of bolt support design for complex roof,” Coal Engineering, vol. 22, pp. 23-24, 2010.

[17] P. Zhao and Z. Yang, “The composite material constitutive model of bedded rocks,” Journal of Lanzhou University, vol. 2, pp. 114-118, 1990.

[18] Z. He, Z. Peng, P. Cao, et al., “Test and numerical simulation for stratified rock mass under uniaxial compression,” Journal of Central South University, vol. 41, no. 5, pp. 1906-1912, 2010.

[19] S. Li, P. Sha, F. Wu, et al., “Analysis of Anisotropic Deformation Characteristics of Layered Rock Mass,” Rock and Soil Mechanics, vol. S2, pp. 366-373, 2018.

[20] C. Chu, S. Wu, S. Zhang, et al., “Mechanical behavior anisotropy and fracture characteristics of bedded sandstone,” Journal of Central South University (Science and Technology), vol. 51, no. 8, pp. 2232-2246, 2020.

[21] C. Wei, X. Wang, X. Yang, et al., “Study on Roof Caving Mechanism and Support Scheme Optimization of Tunnels in Thin-bedded Rock Mass,” Modern Tunnelling Technology, vol. 61, no. 1, pp. 252-259, 2024.

[22] Y. Yang, “Analysis Model of Deformation and Failure Process and Reinforcement Effect of Anchored Layered Rock Mass,” Journal of Rock Mechanics and Engineering, vol. 13, no. 4, pp. 309-317, 1994.

[23] S. Yang, H. Zhu, Z. Liu, “A new constitutive model of the layered rock mass reinforced with bolts,” Chinese Journal of Geotechnical Engineering, vol. 23, no. 4, pp. 427-430, 2001.

[24] J. Zhang and W. Qiu, “Research into Variation Mechanism and Support Measure of Tunnel in Titled Banded Mudstone,” Journal of Highway and Transportation Research and Development, vol. 24, no. 1, pp. 114-117, 2007.

[25] X. Ge, “Study on Shear Strength Performance of Anchored Jointed Surfaces,” Journal of Geotechnical Engineering, vol. 1, pp. 8-19, 1988.

[26] X. Cao, D. Zhou, G. Liu, et al., “Optimization Study on Anchor Support for Shallow-Buried Tunnels in Steeply Dipping Low-Angle Layered Surrounding Rock,” Journal of Underground Space and Engineering, vol. S2, pp. 1926-1930, 2013.

[27] F. Yang, W. Chen, P. Zheng, et al., “Study on the Deformation and Failure Mechanism and Support Technology of Steeply Inclined Soft-Hard Interbedded Tunnels,” Geotechnical Mechanics, vol. 35, no. 8, pp. 2367-2374, 2014.

[28] L. Zhang, L. Chen, J. Chen, et al., “Deformation Characteristics and Treatment Measures of Tunnels in Soft and Hard Interbedded Surrounding Rock with Tilted Stratum,” Journal of Architecture and Civil Engineering, vol. 38, no. 6, pp. 186-196, 2021.

[29] W. Pang, Z. Xia, H. Jiao, “Influence of the Angle between Terrane Strike and Tunnel on the Deformation Characteristics of Surrounding Rock,” Journal of Railway Engineering Society, vol. 36, no. 7, pp. 52-57, 2019.

[30] Q. Guo, “Study on Deformation Control Technology of Soft Hard Interbedded Tunnel with High Ground Stress,” Journal of Railway Engineering Society, vol. 40, no. 9, pp. 72-77, 2023.

[31] W. Wang, S. Han, E. Dong, et al., “Simulation on anchorage mechanism of rock mass,” Journal of China Coal Society, vol. 48, no. 1, pp. 177-184, 2023.

[32] H. Kang, “Analysis of Application Cases of Bolt Support in Coal Mine Roadways,” Journal of Rock Mechanics and Engineering, vol. 29, no. 4, pp. 649-664, 2010.

[33] M. Cai, “Key theories and technologies for surrounding rock stability and ground control in deep mining,” Journal of Mining and Strata Control Engineering, vol. 2, no. 3, pp. 1-9, 2020.

[34] H. Chen, Y. Ye, N. Hu, et al., “Stress characteristics and critical length of bolt in composite roof,” Journal of Mining and Safety Engineering, vol. 37, no. 6, pp. 1162-1170, 2020.

[35] S. Yang and B. Zhang, “Mechanical Nature of the Interaction Between Anchor Bolts and Rock-